

Simulation of cascaded polarization-coupled systems of broad-area semiconductor lasers

M. Radziunas*, J. Montiel-Ponsoda†, G. Garre-Werner‡, and V. Raab‡

*Weierstrass Institute (WIAS), Mohrenstrasse 39, 10117 Berlin, Germany. Email: Mindaugas.Radziunas@wias-berlin.de

†Monocrom S.L., Carrer de la Vilanoveta 6, 08800 Vilanova i la Geltrú, Spain.

‡Raab-Photonik GmbH, Amundsenstr. 10, 14469 Potsdam, Germany.

Abstract—We present a brightness- and power-scalable polarization beam combining scheme for high-power, broad-area semiconductor lasers. To achieve the beam combining, we employ Lyot-filtered optical reinjection from an external cavity, which forces lasing of the individual diodes on interleaved frequency combs with overlapping envelopes and enables a high optical coupling efficiency. We demonstrate how repeatedly introduced new stages of the external cavity allow efficient coupling of 2^n emitters. We simulate the operation of two-four-eight-sixteen coupled emitters, analyze beam coupling efficiency, and discuss possible limiting factors of this coupling scheme.

High-power broad-area edge-emitting semiconductor lasers (BALs) are key devices in many modern applications. By using laser diode arrays and suitable beam combining techniques, one can generate kW-beams which are needed for material processing, for example. In this paper, we analyze a cascaded polarization and spectral beam combining technique that can be employed for coupling BALs with a similar emission wavelength and produces a combined output beam with a well-defined polarization state. For the first experimental demonstration of two emitters coupled according to the scheme analyzed in this paper, see Ref. [1]. Numerical simulations and analysis of this such configuration were done in Ref. [2].

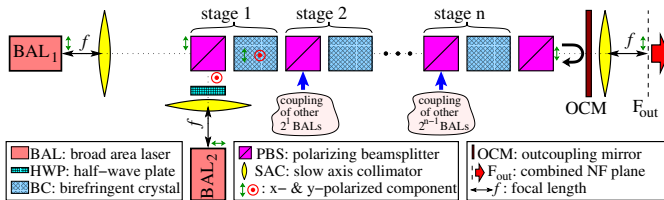


Fig. 1. Schematics of 2^n BALs coupled by the cascaded external cavity with n stages. Coupling of the first two diodes within Stage 1 is shown explicitly.

Setup: In this work, we consider a system of 2^n high-power broad-area semiconductor lasers (BALs) coupled via a cascaded external cavity (EC). It contains different optical elements such as (slow-axis) collimating (SAC) lenses, birefringent crystals (BCs), polarization beam splitters (PBSs), wave-plates (WPs), and a partially reflecting outcoupling mirror (OCM). Fig. 1 gives a schematic representation of this system. For simplicity, this scheme ignores vertical (fast axis) dimension, assuming ideal fast axis collimation by the adequately located lenses (not shown in the scheme). We also assume that the SAC lenses are perfectly perpendicular to the optical axes of each BAL and are located at the focal distance f from the facets of the lasers. One more SAC lens outside the OCM transforms the k_x -space representation of the

optical fields back to the standard space. The superposition of the emitted fields at the focal distance f behind this outer lens (focal plane F_{out} in Fig. 1) composes a combined near-field of all BALs. The diodes are coupled by the EC, which contains cascaded Lyot filters (combinations of PBS, BC, and another PBS), admits a few % field intensity reflection from the OCM, and provides individually filtered optical reinjections to each emitter. Fig. 2 is an example of the mutually interleaved self-reflection spectra implied by a 3-staged EC to each of eight coupled diodes. In the optimal case, the entire reflected field of the individual BAL is reinjected into the emitting diode (dominant self-feedback). In contrast, the cross-feedback vanishes, minimizing in this way the coupling of the diodes.

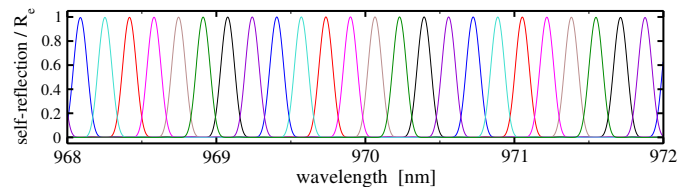


Fig. 2. Intensities of self-reflection as functions of wavelength for eight diodes coupled by the EC. $R_e = 0.04$: intensity reflection of the OCM.

Model: For modeling nonlinear dynamics in BALs, we use a 2(space)+1(time) dimensional traveling wave (TW) model [3] and the electro-optical (EO)-solver BALaser [4]. The model is based on the TW equations for the slowly varying complex amplitudes of the counter-propagating TE-polarized fields $E_j^\pm(z, x, t)$ within the active zone of each BAL_j :

$$\left[\frac{1}{v_g} \partial_t \pm \partial_z + \frac{i}{2\bar{n}k_0} \partial_x^2 \right] E_j^\pm = -i\beta(N, E^\pm, T)E_j^\pm + F_{sp}^\pm. \quad (1)$$

Here v_g , k_0 , \bar{n} , and F_{sp}^\pm are the group velocity of light, the free-space central wavenumber, the reference refractive index, and the Langevin noise, respectively. The complex factor β accounts for absorption, an induced refractive index profile, material gain, and refractive index. The last two factors depend on the local carrier density $N_j(z, x, t)$ and account for nonlinear gain compression and material gain dispersion. The diffusive (in x) rate equation governs the dynamics of N [3]. To determine carrier diffusion and injected current, we simultaneously solve the carrier spreading problem in lateral/vertical (x/y) cross-sections of the BALs [5]. Moreover, we alternate ~ 5 ns transient simulations of the EO model described above with the solution of the static heat-flow model for 3-dimensional time-averaged temperature distribution in the diodes, which determines the heating-induced corrections

to the refractive index and some other model parameters [6]. At the lateral borders of the (sufficiently broad) computational domain, we impose periodic conditions on E_j^\pm and N_j . At the high-reflecting rear facets, $z = 0$, reflecting conditions $E_j^+(0, x, t) = \sqrt{R_0}E_j^-(0, x, t)$ hold. Finally, at the low-reflecting front facet, $z = l$, facing the EC, we have another reflecting condition with an additional reinjection from the EC:

$$\begin{aligned} E_j^-(l, x, t) &= \sqrt{R_l}E_j^+(l, x, t) + t_l E_j^r(x, t), \\ E_j^r(x, t) &= \sum_{k=1}^{2^n} [M_{[j,k]} E_k^e](x, t). \end{aligned} \quad (2)$$

$R_0 \lesssim 1$, $R_l \ll 1$, and $t_l = \sqrt{1 - R_l}$ are field intensity reflections and amplitude transmission at the corresponding facet. E_j^r and $E_j^e(x, t) = t_l E^+(l, x, t)$ are reinjected and emitted x -polarized fields just outside the front facet of BAL $_j$. The combined beam at the F_{out} plane behind the OCM (see Fig. 1) is given by

$$E^c(x, t) = \sum_{j=1}^{2^n} E_j^c(x, t), \quad E_j^c = [M_{[j]} E_k^e](x, t). \quad (3)$$

The scalar operators $M_{[j,k]}$ and $M_{[j]}$ are the upper left elements of 2×2 -dimensional matrix operators $\mathbf{M}_{[j,k]}$ and $\mathbf{M}_{[j]}$ translating the (x - and y - polarized) vector-field $\mathbf{E} = \begin{pmatrix} E_x \\ E_y \end{pmatrix}$ from BAL $_k$ to BAL $_r$ or to F_{out} plane, respectively. Both vector-field components are interchanging within BCs and WPs. The configuration of the EC, however, implies vanishing of all but upper-left components of $\mathbf{M}_{[j,k]}$ and $\mathbf{M}_{[j]}$, such that optical feedback and combined beams are x -polarized. For the construction of efficient models, we used a paraxial approximation of the wave equations. Moreover, we neglected differences of optical pathlengths and backscattering from all (antireflection coated) elements of the EC, used an idealized thin lens model, and assumed perfect polarization splitting in PBSs. The resulting local in time and space operators $M_{[j,k]}$ and $M_{[j]}$ could be efficiently integrated into our solver. They are sums of several telescope-type operators, which induce different time delays, phase shifts, and swap of the coordinate x . These operators for two coupled diodes are given in Ref. [2]. The case of arbitrary n will be described elsewhere.

Simulations: We have simulated spatiotemporal dynamics of one or 2/4/8/16 coupled diodes, each operating at 970 nm and emitting ~ 12 W. All identically driven diodes were 4 mm long, had $100 \mu\text{m}$ -broad contacts, and $5 \mu\text{m}$ -wide refractive index trenches nearby. The 4 mm - long BCs (calcite) within the first stage of the EC defines ~ 1.3 nm wavelength-periodicity of the Lyot filters, see Figs. 2 and 3(a). For more details on the laser and EC parameters, see Ref. [2] and references therein. We assume that all elements within the EC are lossless and perfectly positioned. The field losses in the EC are only due to imperfect filtering-induced optical mode selection in individual BALs. Part of the emitted modes with the wavelengths deviating from the maximal spectral filtering positions, see Fig. 2, generate different polarization components at the end of BCs and are not entirely bypassing the following PBS on their way to the OCM. Individual interleaving optical spectra, near- and far-fields, as well as scaled coupled beams of different laser configurations, are shown in Fig. 3. The coupling scheme induces only a slight broadening of spectral, spatial, and angular characteristics of the combined beam, comparing them to those characteristics of the single BAL (upper diagrams in Fig. 3). The combined beam power upscales with the number of diodes and is proportional to the coupling efficiency factor $\eta = \sum_j^{2^n} P_j^c / P_0^{(n)}$. Here P_j^c

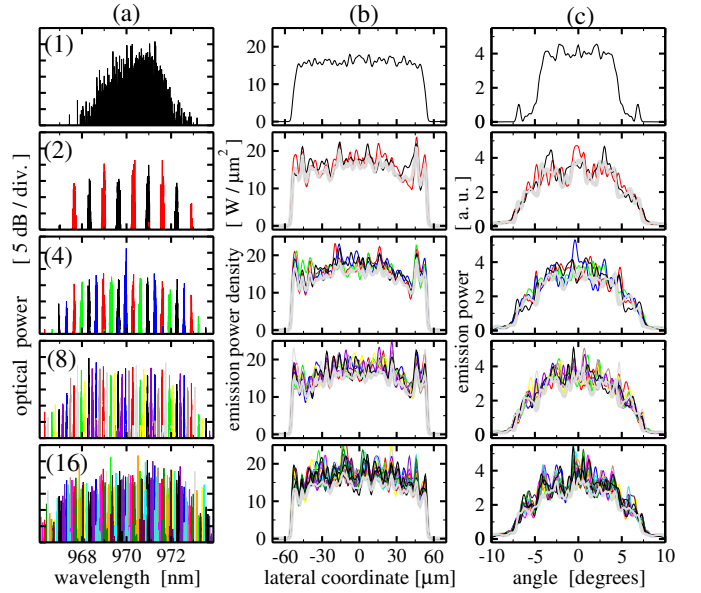


Fig. 3. Simulations of the single diode without feedback (1) and 2/4/8/16 coupled BALs (corresponding lower rows). Thin lines: optical spectra (a) and field intensities (b) of the individual diode emission at the front facet, as well as corresponding far fields (c). Thick grey in (b) and (c): representations of the combined beam (divided by the number of emitters) at the F_{out} plane.

and $P_0^{(n)}$ are the time-averaged power of the combined beam component E_j^c and cumulative power of the fields E_j^e at the front facets of all 2^n diodes. Power P_0 at the facets and efficiency η for considered configurations are collected in Table I. The efficiency shows about 2% decay with each additional coupling stage but still can reach 86% for 16 emitters.

TABLE I. OPERATION OF BALs COUPLED BY THE LOSSLESS EC.

	1 BAL w/o feedback	2 BALs	4 BALs	8 BALs	16 BALs
P_0 [W]	11.8360	25.1428	49.9095	100.0206	198.5452
η		0.9270	0.8934	0.8879	0.8600

In conclusion, we discussed a quality-preserving beam-combining scheme for 2^n emitters showing $\sim 90\%$ coupling efficiency. With each new coupling stage, the efficiency decays by $\sim 2\%$. The efficiencies calculated in this work for idealized EC are well above those of $\leq 80\%$ reported for two coupled laser bars in the experimental system [2]. We have repeated several simulations assuming 4% intensity loss within each coupling stage. The efficiency dropped to 89% and 72% in two- and sixteen-coupled-diode cases, respectively. Thus, one of the biggest challenges when constructing the above-discussed systems is minimizing the field losses in the EC.

Acknowledgment: This work was supported by the EUROSTARS Project E!10524 HIP-Lasers.

REFERENCES

- [1] V. Raab and C. Raab, *Zeitschrift Photonik*, **5**(5), 46-49, 2004.
- [2] C. Bree et al., *J. Opt. Soc. Am. B*, **36**(7), 1721-1730, 2019.
- [3] M. Radziunas, *The Int. J. of High Perf. Comp. Appl.*, **32**, 512-522, 2018.
- [4] "BALaser: a software tool for simulation of dynamics in Broad Area semiconductor Lasers," <http://www.wias-berlin.de/software/BALaser>.
- [5] M. Radziunas et al., *Optical and Quantum Electronics*, **49**, 332, 2017.
- [6] M. Radziunas et al., *Optical and Quantum Electronics*, **51**, 69, 2019.